evs30

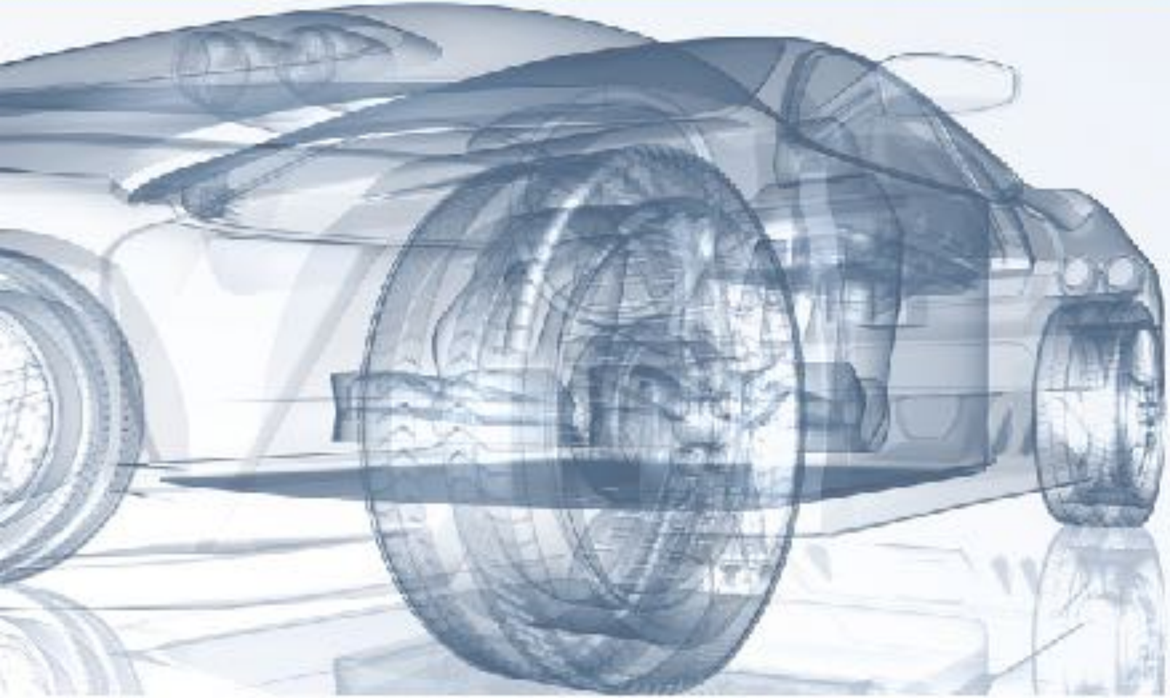

# The 30th International Electric Vehicle Symposium & Exhibition

## October 9–11, 2017

Messe Stuttgart, Germany

www.evs30.org

# Operating Point Adaptation for NVH-Optimization of Induction Machines

W. M. Bischof, F. Draeger, M. D. Hennen, R. M. Kennel

Tuesday, October 10., 2017

# Agenda

- Introduction
- Theoretical Background
- Acoustic Measurements
- Calculation of the Operating Points
- Validation of the Optimization
- Conclusion

- *Using induction machines, several different operating points for the same torque are possible*
- *Operating points are normally optimized in regard to efficiency of machine or drive system*
- *Operating points have influence on force excitation and subsequently vibrations and audible noises*
- *Analysis of an NVH operating strategy with pre-investigations in 3 operating points:*
  → *Minimum flux, reference flux, maximum flux*

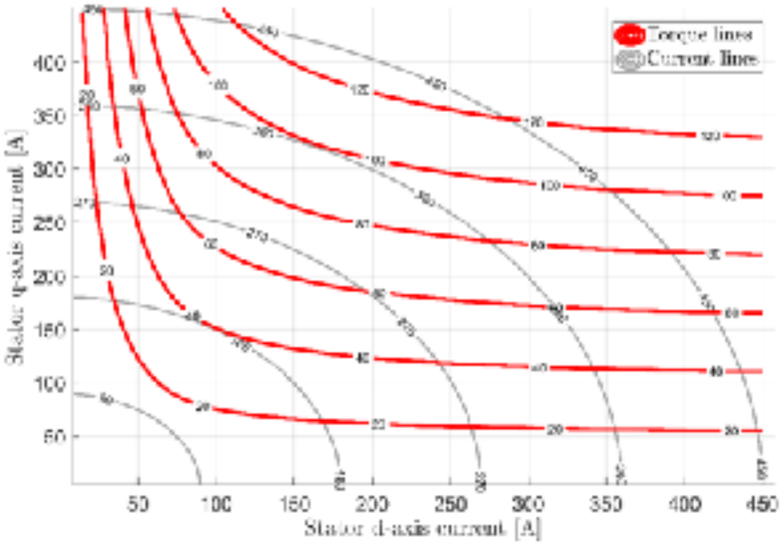


**Source: [1, 2, 3, 5, 9, 10]**

# Introduction

- ***Using induction machines, several different operating points for the same torque are possible***

- ***Operating points are normally optimized in regard to efficiency of machine or drive system***

- ***Operating points have influence on force excitation and subsequently vibrations and audible noises***

- ***Analysis of an NVH operating strategy with pre-investigations in 3 operating points:***
  ***→ Minimum flux, reference flux, maximum flux***

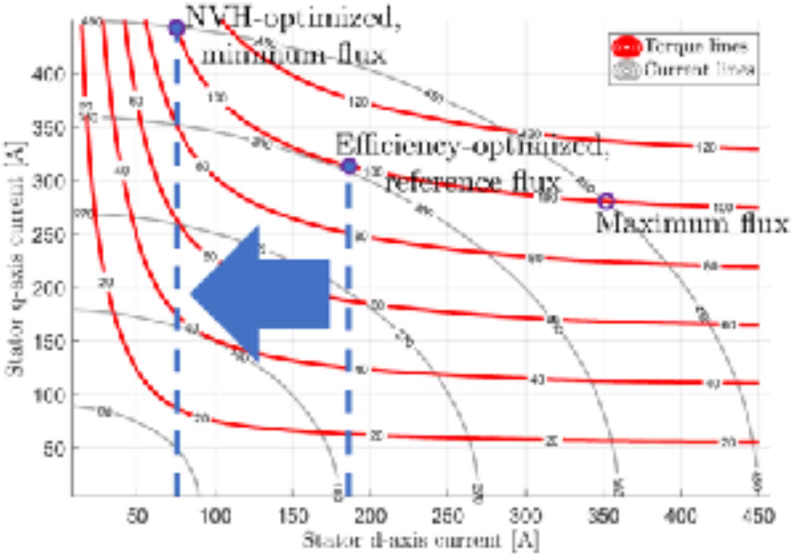


***Source: [1, 2, 3, 5, 9, 10]***

## *Theoretical Background*

- ***Investigation in the induction machines fundamental behavior***

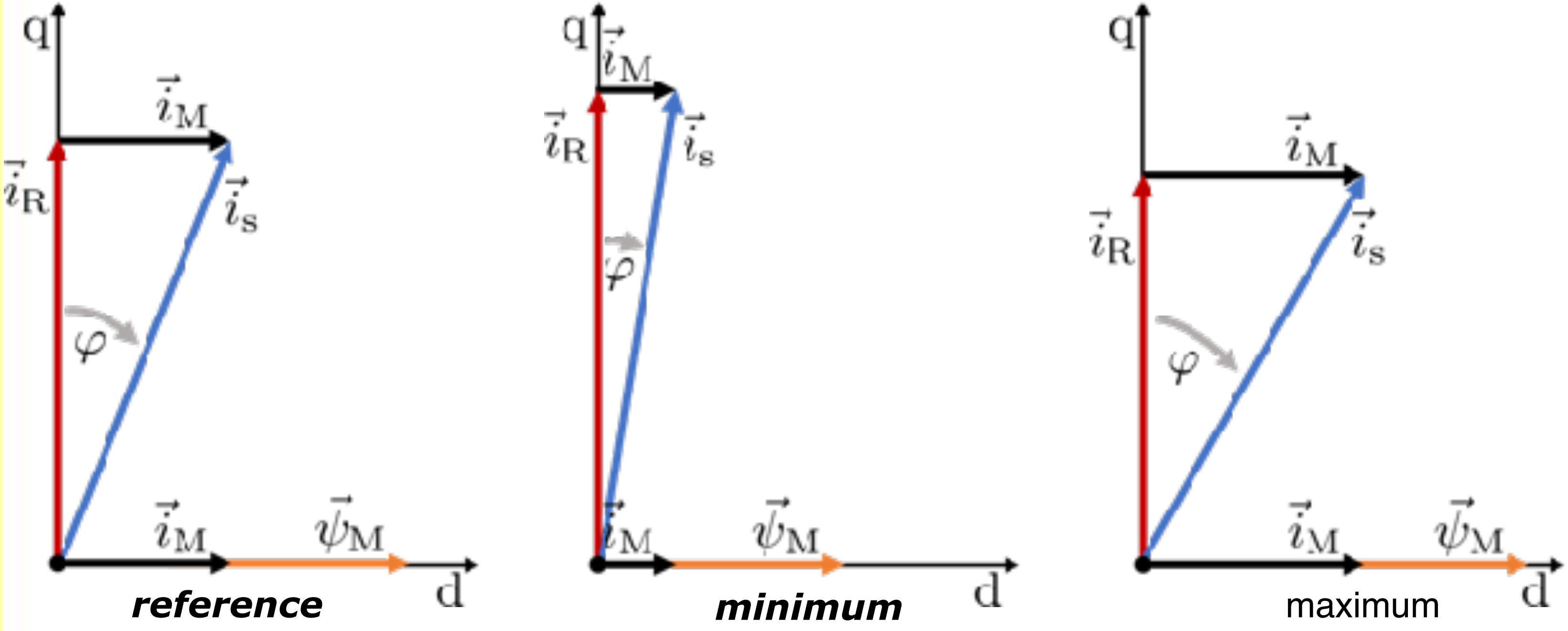


$$\varphi(I_{\mathrm{d,min}}) \leq \varphi(I_{\mathrm{d,ref}}) \leq \varphi(I_{\mathrm{d,max}})$$

- ***Considering the spatial and temporal harmonics of the magneto motive forces***
- ***Rough estimation of magnetic forces***

$$F_{\mathrm{r}}(\alpha,t) = \frac{B^2_{\mathrm{air-gap}}(\alpha,t)}{2\mu_0} A_{\mathrm{surf}}$$

$$B_{\mathrm{air-gap}}(\alpha,t) = \underbrace{(\Theta_{\mathrm{s}}(\alpha,t) + \Theta_{\mathrm{r}}(\alpha,t))}_{\Theta(\alpha,t)} \Lambda_{\mathrm{air-gap}}(\alpha,t)$$

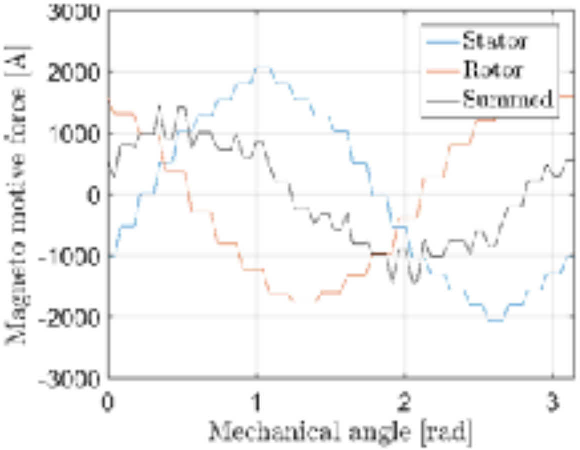


***reference***

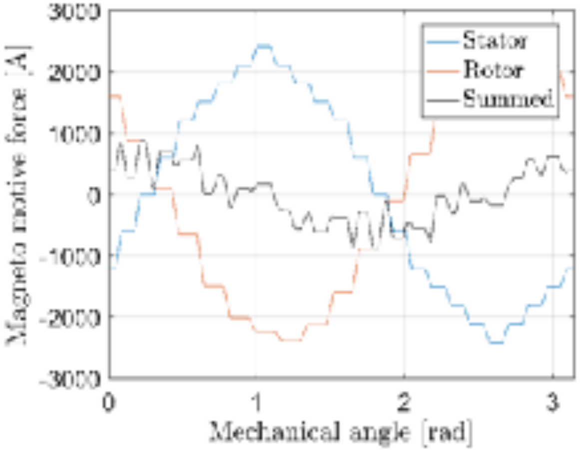


***minimum***

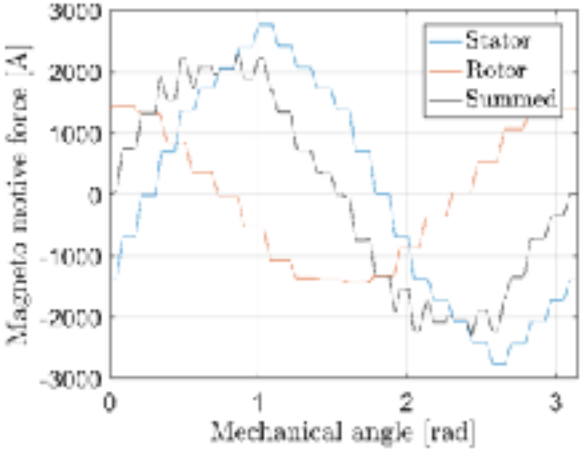


maximum

$$\vec{i}_{\mathrm{s}}(t) \propto \Theta_{\mathrm{s}}(\alpha,t), \vec{i}_{\mathrm{R}}(t) \propto \Theta_{\mathrm{r}}(\alpha,t), \vec{i}_{\mathrm{M}}(t) \propto \Theta(\alpha,t) \text{ and } \vec{\psi}_{\mathrm{M}}(t) \propto B_{\mathrm{air-gap}}(\alpha,t).$$

## Theoretical Background

- ***Simulation of radial forces for 60Nm of torque***

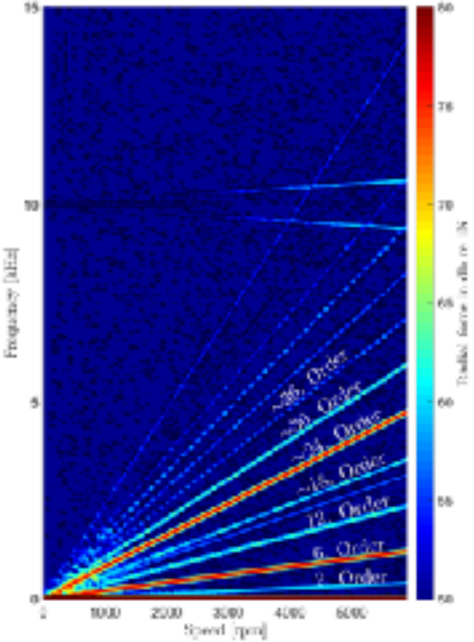

***reference***

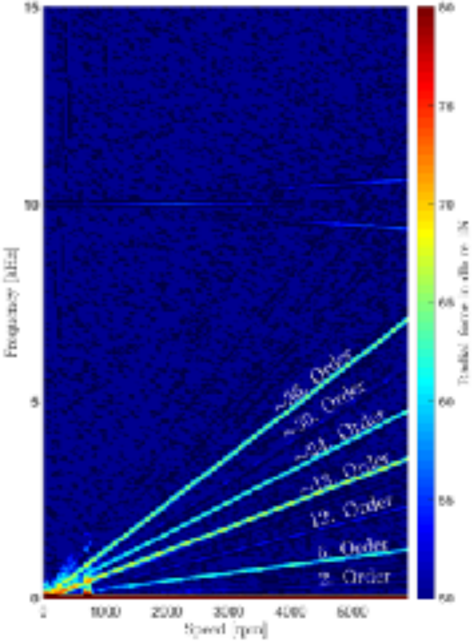

***minimum***

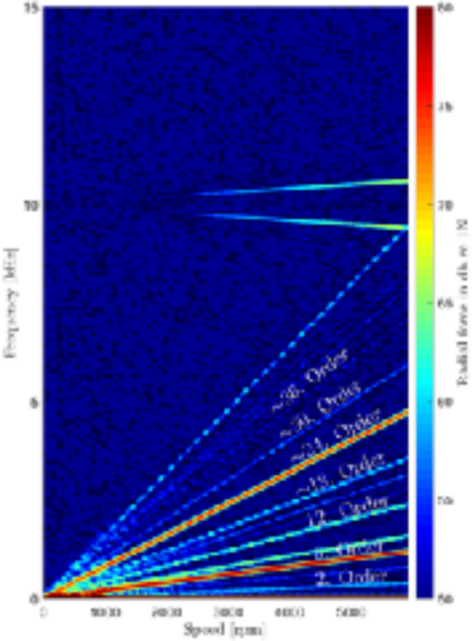

maximum

Harmonic stimulation changes with machine opertating point

## *Theoretical Background*

- ***The radial forces with minimum flux show the lowes mean force level on the stator tooth***

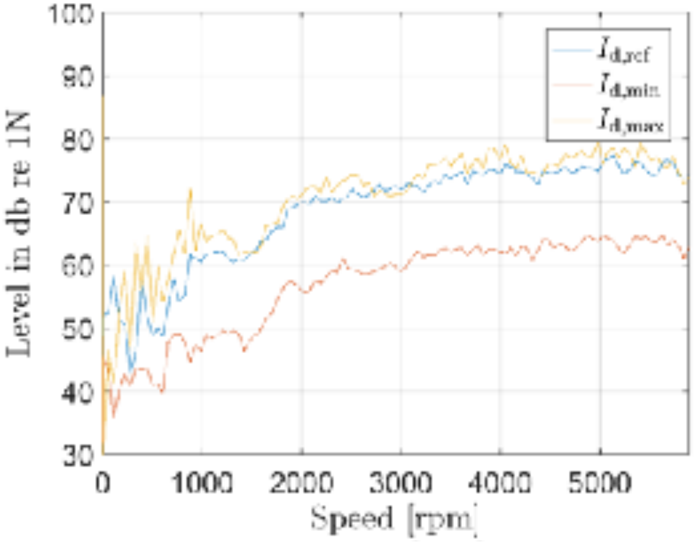


- ***Damping of the stator structural dynamics has to be considered changing the dominance of force harmonics***

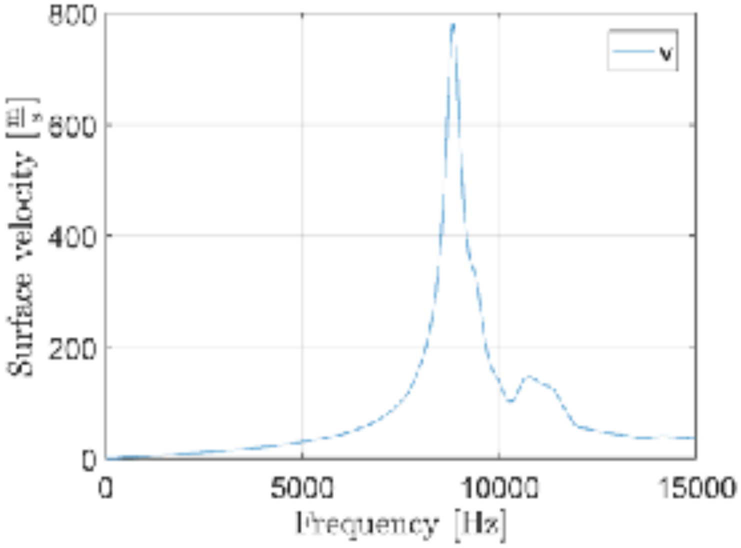

## *Acoustic Measurements*

$$|\bar{v}_{\mathrm{r}}(t)|^2 = \frac{1}{2\pi}\int_0^{2\pi} |v_{\mathrm{r}}(\alpha, t)|^2 \mathrm{d}\alpha$$

- ***Measurements of the surface velocity for 60Nm of torque***

$$P(t) \propto |\bar{v}_{\mathrm{r}}(t)|^2$$

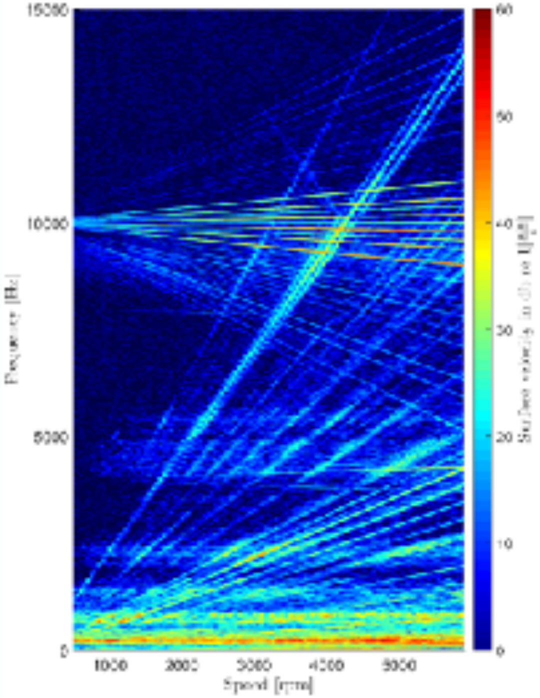


***reference***

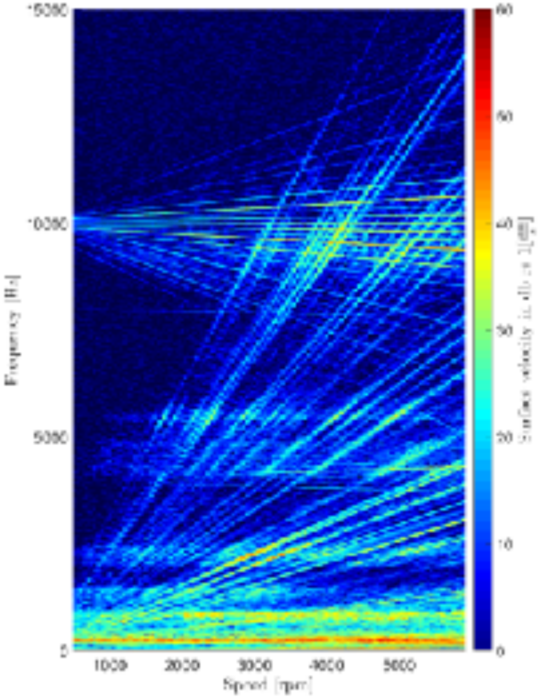


***minimum***

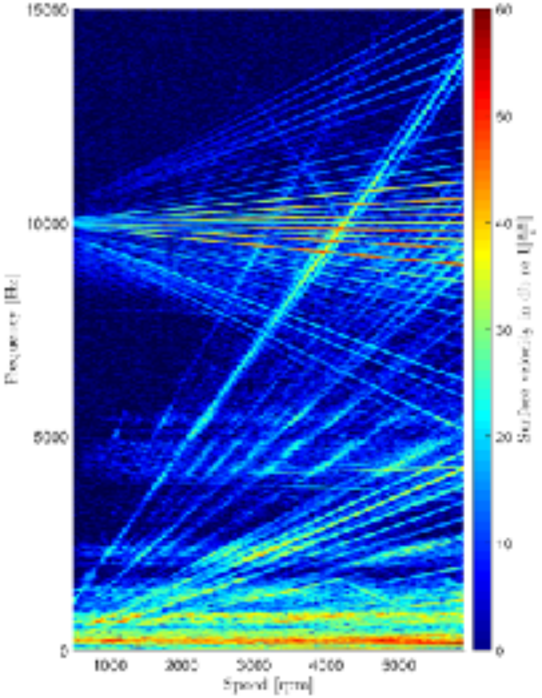


maximum

## *Acoustic Measurements*

- ***Comparison of speed run-ups at 20Nm, 60Nm and 100Nm of torque***
- ***Surface velocity levels are rated with an A weighting curve***

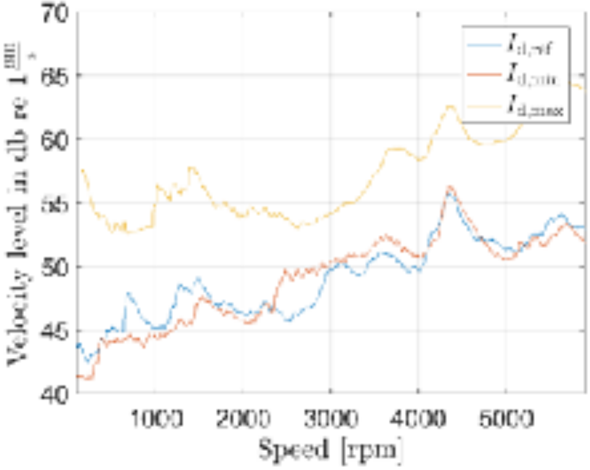


20Nm

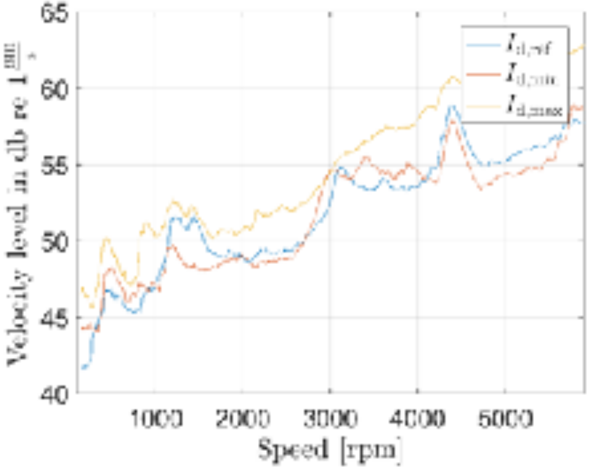


60Nm

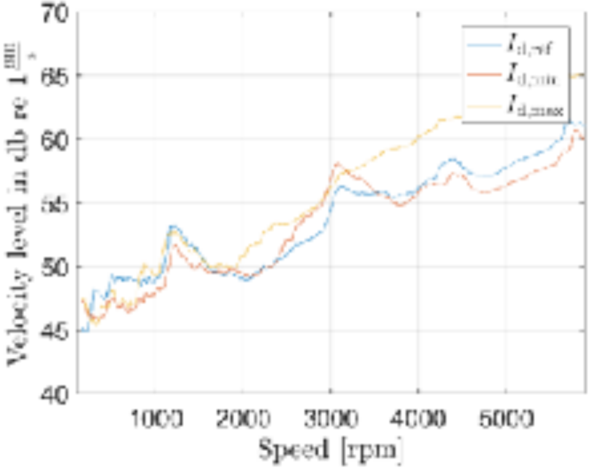


100Nm

Potential of noise optimization increases with increasing torque

## *Acoustic Measurements*

- ***Comparison of speed run-ups at 20Nm, 60Nm and 100Nm of torque***
- ***Surface velocity levels are rated with an A weighting curve***
- ***Maximum difference of all measured velocity levels***

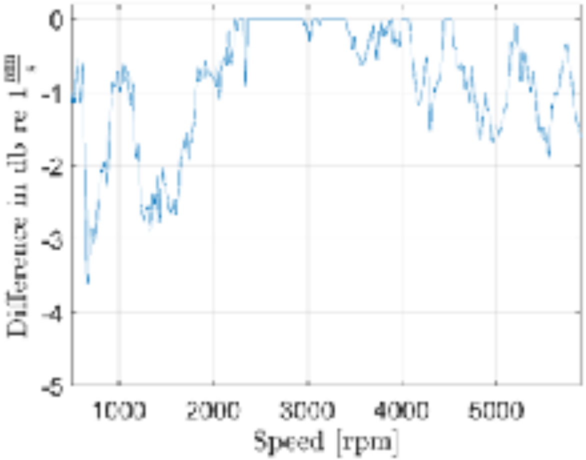


20Nm

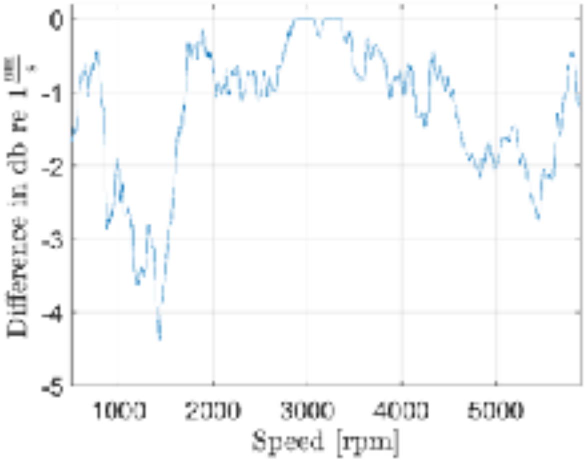


60Nm

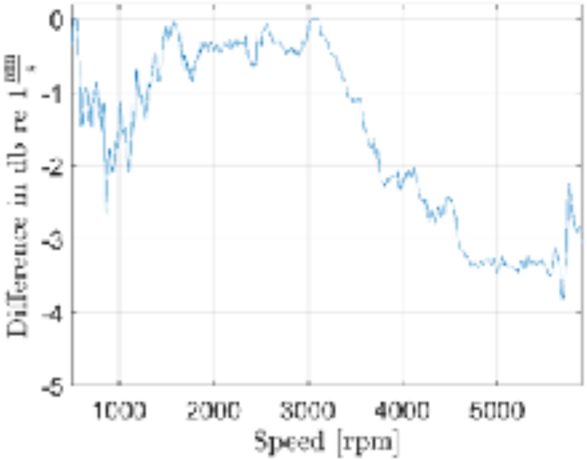


100Nm

Potential of up to 4 dB noise reduction

## Calculation of the Operating Points

- NVH-optimized operating strategy mainly in minimum flux region

➔ Maximum stator current at complete torque region

- NVH-optimized points are far away from optimum efficiency points

➔NVH-optimization has a huge influence on e-drive efficiency

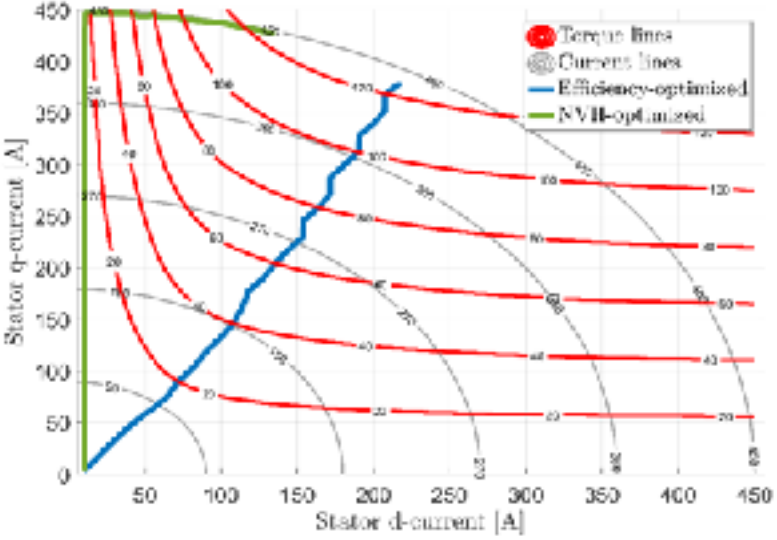


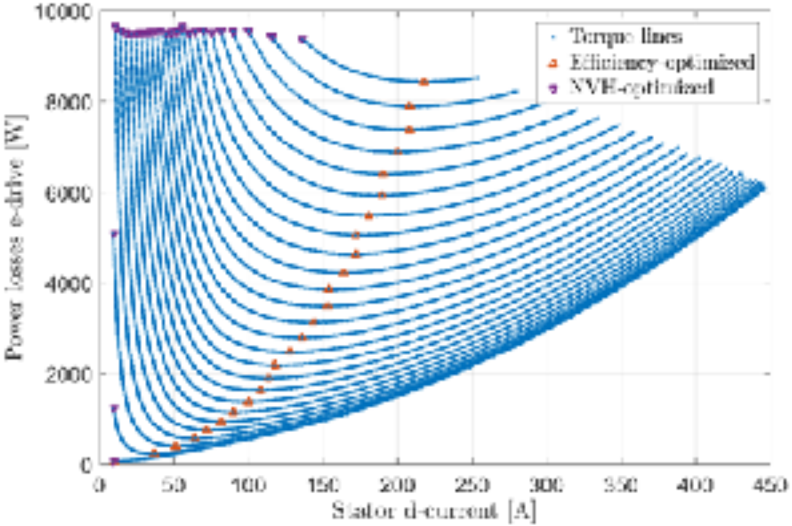

## *Calculation of the Operating Points*

- ***The optimized strategy determines the operating point depending on desired torque and speed of the e-drive.***
- ***Optimization criteria is defined to switch from best efficiency to NVH-optimized operation at an improvement of 20%***
- ***Reducing number of switching by holding the state in a range of 5%***

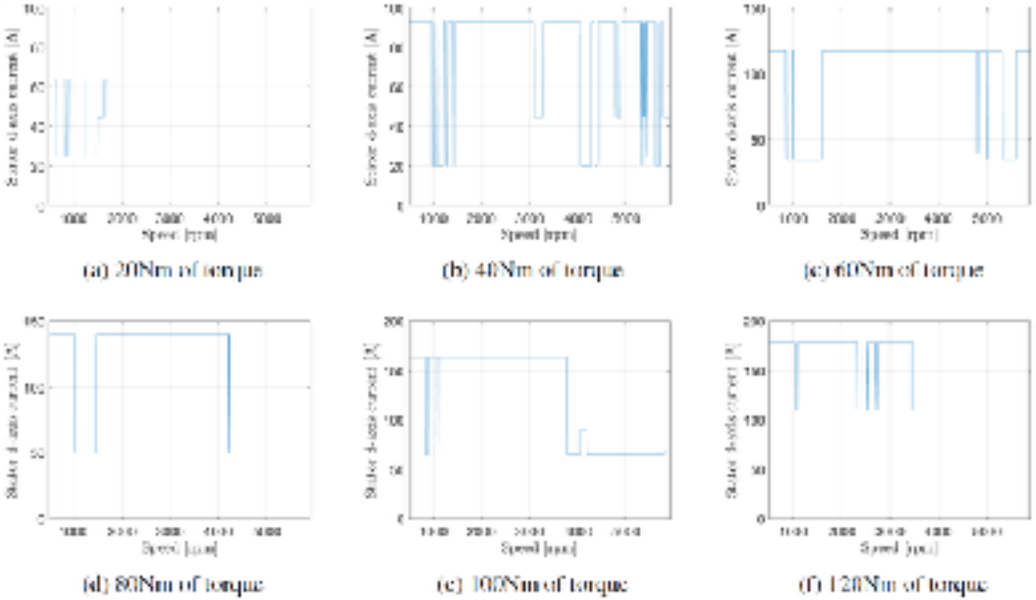


Figure 14: Stator d-axis current for noise optimized operating at a) 20Nm, b) 40Nm, c) 60Nm, d) 80Nm, e) 100Nm and f) 120Nm of torque.

Optimization criteria:

$$I_d(t) = \begin{cases} I_{d,eff}(t) & \text{, if } \min(v_r(\alpha,t)) > v_r(\alpha, I_{d,opt}(t)) + 2dB \\ I_{d,opt}(t) & \text{, if } \min(v_r(\alpha,t)) = v_r(\alpha, I_{d,opt}(t)) + 2dB \end{cases}$$

# Validation of the Optimization

- Validation with surface velocity measurement speed run-ups at 40Nm of torque
- Because of controller and temperature influences, velocity levels till 2500 rpm are not matching
- Noises are reduced by more than 3dB

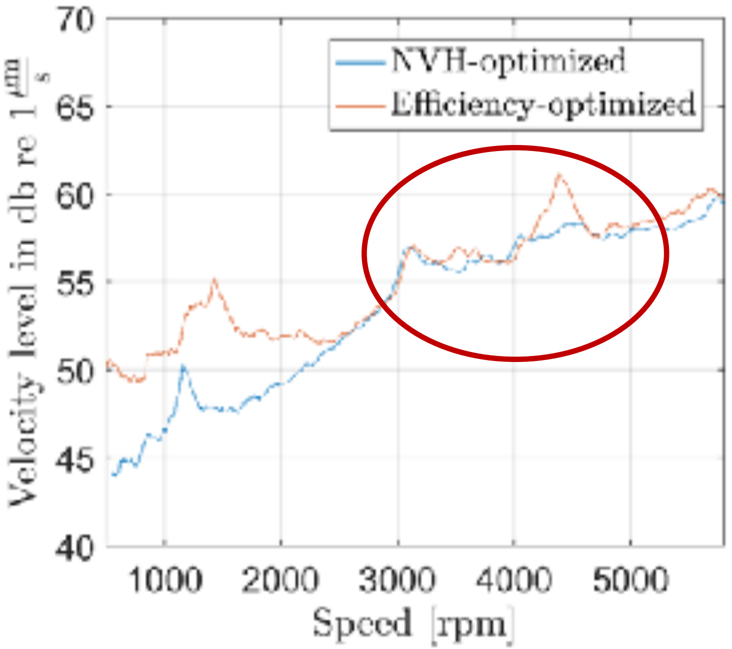

# Conclusion

- *Cause effect relationship is validated*
- *Optimization is operable for different torque and speed operating points*
- *Procedure is performable in the fundamental speed range*
- *Operation Points with best efficiency are left, which can cause thermal issues*
- *Huge influence of stator and rotor temperature complicates the NVH-optimization*

**Future Work:**

- *Optimization strategy is extendable for driver profiles, driving cycles and customer requirements*
- *Extension for temperature dependency*
- *Investigation NVH-optimization in field weakening area*

## References


[1] J. Le Besnerais, Reduction of magnetic noise in PWM-supplied induction machines low-noise design rules and multi-objective optimization, Diss. Ecole Centrale de Lille, Laboratoire dEletcricit et dElectronique de Puissance, 2008.

[2] W. M. Bischof, M. D. Hennen, and R. M. Kennel, Synthesized Magnetic Flux Density in Three-Phase Cage Induction Machines with MATLAB & Simulink, in 18th International Conference on Electrical Machines and Systems (ICEMS), 2015.

[3] W. M. Bischof, B. Chatterjee, M. Boesing, M. D. Hennen, and R. M. Kennel, Modeling Radial Air-Gap Forces of Three-Phase Cage Induction Machines in Spatial Frequency Domain, in 19th International Conference on Electrical Machines and Systems (ICEMS), 2016.

[4] M. Bösing, Acoustic Modeling of Electrical Drives RWTH Aachen, Diss. Institut für Stromrichtertechnik und Elektrische Antriebe, RWTH Aachen, 2013.

[5] W. M. Bischof, B. Chatterjee, M. Boesing, M. D. Hennen, and R. M. Kennel, Modeling Inverter-Fed Three-Phase Squirrel-Cage Induction Machines including Spatial and Temporal Harmonics, in International Electric Machines and Drives Conference (IEMDC), 2017.

[6] R. De Doncker, D. W. Pulle, and A. Veltman, Advanced Electrical Drives - Analysis, Modeling, Control, 1st ed. Dordrecht, NL: Springer Science+Business Media B.V., 2011.

[7] G. Müller, K. Vogt and B. Ponick, Berechnung elektrischer Maschinen, Wannheim, D: WILEY-VCH Verlag GmbH & Co. KGaA, 2008.

[8] G. Müller and B. Ponick, Theorie elektrischer Maschinen, Wannheim, D: WILEY-VCH Verlag GmbH & Co. KGaA, 2009.

[9] P. Kotter, C. Koepf, W. M. Bischof, K. Wegener, Efficient Noise-Vibration-Harshness-modeling for squirrelcage induction drives in EV

**Thank you very much for your attention!**